PHYSICAL REVIEW C VOLUME 7, NUMBER 4 APRIL 1973

Exchange Interpretation of the Large-Angle Scattering of Alpha Particles from Nuclei*

D. Agassi†

Center for Theoretical Physics and Department of Physics and Astronomy, University of Maryland, College Park, Maryland 20742, and Department of Nuclear Physics, Weizmann Institute, Rehovot, Israel

and

N. S. Wall‡

Center for Theoretical Physics and Department of Physics and Astronomy, University of Maryland, College Park, Maryland 20742

(Received 12 June 1972)

The anomalous large-angle scattering of medium-energy α particles is interpreted in terms of an exchange process. An exchange amplitude ("knock on"), calculated in the distorted-wave Born approximation, is evaluated paying particular attention to the antisymmetrization of the $A+4$ nucleon system. This amplitude is combined with a scattering matrix appropriate to fit just forward-angle elastic scattering. It is shown that only the highest possible orbital angular momentum cluster ($L=8$ for ^{40}Ca) is significant and leads to agreement with experiment. This agreement is achieved with only one adjustable parameter, the spectroscopic factor, which turns out to be quite small. It is shown that this microscopic caluclation may provide a basis for the phenomenological Regge pole description of this process.

I. INTRODUCTION

The so-called anomalous large-angle α-particle scattering effect (ALAS) has, by now, been observed in a number of different light and medium nuclei at various energies.[1-4] In elastic scattering and at forward angles one observes a well-understood diffraction pattern. On the basis of scattering from diffuse, strongly absorbing nuclei one would expect an oscillatory pattern which is strongly decreasing as well as damped out at large angles. The ALAS on the other hand demonstrates a forward-angle diffraction pattern, but at large angles a strong oscillation and generally increasing differential cross section is observed.

The ALAS has generated considerable interest as a process that might shed light on α clustering in the vicinity of the nuclear surface. There have been many "explanations" [5-15] for the ALAS without any apparent connection among them. A straightforward attempt to perform an optical-model (OM) fit has been successful in one case,[15] but in general such a simple analysis does not seem to work.[16,17] Various attempts to explain or simulate ALAS have tried to enhance one or a few particular partial waves, based on the following argument. For a $J=0$ nucleus the α-particle elastic scattering amplitude, $f(\theta)$, is given by

$$f(\theta)=f_c(\theta)+\frac{1}{2ik}\sum_{l=0}^{\infty}(2l+1)e^{2i\sigma_l}(\eta_l-1)P_l(\cos\theta)\,, \tag{I.1}$$

where $f_c(\theta)$ is the Coulomb amplitude and σ_l are the Coulomb phase shifts. All other symbols have their usual meaning.[18] The η_l giving rise to the usual diffraction pattern are small for the strongly absorbed low partial waves and rise smoothly with a width of at most only a few units in l centered near $l_0 \sim kR$ where R is the nuclear radius. For large l, η_l goes to unity. At angles near 180° the adjacent Legendre polynomials differ in sign and this is largely responsible for the damping as well as the over-all decrease in the differential cross section. If, however, one partial wave is particularly accentuated, relative to the smoothly varying η_l, then at large angles that one partial wave, L_0, will contribute to the cross section a term roughly proportional to $|P_{L_0}(\cos\theta)|^2$. At forward angles this one term does not dominate because of the presence of Coulomb scattering and the fact that all partial-wave amplitudes are of the same sign. An "l spike" could then contribute an additional amplitude to Eq. (I.1) of the form

$$\Delta f_N=\frac{1}{2ik}\sum_{l=0}^{\infty}(2l+1)e^{2i\sigma_l}a_lP_l(\cos\theta)\,, \tag{I.2}$$

where the a_l amplitudes are peaked in l to form the desired accentuated partial waves.

The main criticism of most of the ALAS explanations is simply that the spike is introduced only phenomenologically with no quantitative, "microscopic," basis. One calculation, by Noble and Coelho[10] similar in spirit to the present work attempts to modify the elastic scattering by adding an amplitude arising from heavy-particle stripping (HPS) for the case of α particles incident on ^{16}O. The present work suggests that the "knock-on" (KO) exchange process[18] is an important term in generating a_l. In this calculation we perform a distorted-wave Born-approximation (DWBA) calculation for the additional amplitude. To obtain

the DWBA amplitude we generate distorted waves from an OM analysis of the *forward-angle scattering*, and we treat fully the antisymmetrization involved.

That such a process produces an a_l which is surface peaked is a very general result following arguments of Frahn and Venter[19] and Dar and Kozlowski.[20] If α clusters do exist on the nuclear surface the incident α particle can knock out a cluster moving in the average field of the passive core. On the other hand α clusters from deep inside the nucleus cannot contribute to the KO process, both because clusters are not likely to exist there, and because if they did the incident and outgoing α particles would be strongly absorbed. At large radii the overlap of the incident and bound α particles is small. Therefore, the KO amplitude peaks in coordinate space in the vicinity of the nuclear radius and by semiclassical arguments will therefore exhibit l peaking near $l_0 = kR$.

We shall show that the present model does predict the required spike with an amplitude that reflects the cluster spectroscopic factor. This spike when added to the optical contribution produces the qualitatively correct angular dependence over the entire angular range, not just large angles. The model is consistent with the energy variations of the ALAS as well as its disappearance at high energy.[1,21]

In Sec. II we identify the KO matrix element, introduce the approximations that define the model, and display the specific equations for a_l. Section III is devoted to a presentation of the results obtained for ^{40}Ca and a comparison with experiment. In Sec. IV we compare the various other explanations of ALAS indicating the connection to the present model. Section V presents our conclusions.

II. "KNOCK-ON" MODEL

In this section we first define the KO matrix element and give intuitive arguments for its choice. In order to actually compute the matrix element, further approximations are then introduced and a tractable expression for the a_l is obtained. We then discuss, qualitatively, our expression for a_l to demonstrate its l peaking. Special attention is given throughout to the Pauli principle which is of particular relevance for exchange processes.[18]

Since α particles are strongly absorbed, presumably the direct reaction mechanism is adequate to describe their scattering properly. We choose a DWBA representation to describe the KO process and believe it to be justified for strongly absorbed particles in much the same fashion as it is applied to inelastic α-particle scattering. That is the strong absorption is an indication that many channels are available and the one particular channel we are evaluating represents only a small part of the cross section, enabling a perturbation treatment. In our language a_l should be "small" but to calculate the total *elastic* scattering amplitude we need both a_l and η_l, even though the α_l are small and span a small region of l. This point of view is supported by the "phenomenological" spike, which turns out to be small compared to the $l \sim kR$ amplitude, η_{l_0}.[1] It also suggests that the contribution to the total reaction cross section caused by the introduction of this term should be small. Under these conditions the double counting error inherent in this kind of DWBA analysis will also be small. It should be emphasized that we are applying DWBA to essentially only the high-partial-wave-exchange processes.

For composite particle scattering by a target there are many exchange processes in addition to the direct term. The present interpretation attributes the ALAS to the KO term solely. Two reasons lead to this choice. First the α particle is a particularly stable cluster, and exchange processes in which only a part of the cluster is exchanged and recombines with a suitable fraction of the target to form the outgoing α, are expected to be small. The stability of the α particle is manifest in our treatment by the neglect of excitation of either the incident or outgoing α particle. Secondly, the antisymmetrization results in relatively small combinatorial factors that multiply the corresponding amplitudes, as we shall show later. There are suggestions that "core-exchange" amplitudes should be small.[18] We have not evaluated such amplitudes and the general features of our agreement with experiments suggests these contributions are not important.

The scattering amplitude for a spin-0-charged object on a $J=0$ target is given by Eq. (I.1). For forward angles say $\theta \leq 60°$, where α scattering displays a diffraction pattern, the η_l can be obtained from an OM fit, and are hereafter denoted by $\eta_l^{(\mathrm{opt})}$. This fitting procedure takes into account the direct term as mentioned above. The KO term, to be added to the OM amplitude, represents a perturbation $\Delta f_N(\theta)$ which can be expanded, similarly, in partial waves

$$\Delta f_N = \frac{1}{2ik} \sum_{l=0}^{\infty} (2l+1) e^{2i\sigma_l} a_l P_l(\cos\theta) \qquad \text{(I.2)}$$

such that the total nuclear amplitude valid for all angles is

$$f_N = f_N^{\text{opt}} + \Delta f_N = f_c + \frac{1}{2ik}\sum_{l=0}^{\infty}(2l+1)e^{2i\sigma_l}(\eta_l^{(\text{opt})} + a_l - 1)P_l(\cos\theta)\,. \tag{II.1}$$

The antisymmetrized T matrix element for the reaction $a+\alpha \to b+\beta$ in the DWBA is given[18] by

$$T_{\alpha\beta} = \sum_P (-1)^P \langle \Psi_b \Psi_\beta \chi^{(-)}(\vec{r}_\beta, \vec{k}_\beta), [V_\beta - U_\beta] P \Psi_a \Psi_\alpha \chi^{(+)}(\vec{r}_\alpha, \vec{k}_\alpha)\rangle\,, \tag{II.2}$$

where $\chi_\alpha^{(-)}, \chi_\beta^{(+)}$ are distorted waves in the incoming and outgoing channels α and β, respectively, and depend on the distance between the center of masses of the two fragments involved. Let us assume for simplicity one kind of particle numbered by 1 to N. The α, β channels are chosen to correspond to the partitions

$$\begin{aligned}
&\Psi_a = \Psi_a(1, 2, 3, \ldots, n_a)\,,\\
&\Psi_\alpha = \Psi_\alpha(n_a+1, n_a+2, \ldots, n_a+n_A)\,,\\
&\Psi_b = \Psi_b(1, 2, \ldots, n_b)\,,\\
&\Psi_\beta = \Psi_\beta(n_b+1, \ldots, n_b+n_B)\,,
\end{aligned} \tag{II.3}$$

where the Ψ are antisymmetrized with respect to their specific coordinates, and the operator P realizes all possible permutations between the coordinates of Ψ_a and Ψ_α. There are altogether $\binom{n_a+n_A}{n_a}$ such permutations. The sign $(-1)^P$ is positive if an even number of particles are exchanged, and negative for an odd number of particles. The phenomenological optical potential U_β depends only on $\vec{r}_\beta$, whereas the residual interaction $V(i,j)$ leads to,

$$V_\beta = \sum_{\substack{i=1,\ldots,n_b \\ j=n_b+1,\ldots,n_b+n_B}} V(i,j)\,. \tag{II.4}$$

It is now a simple exercise to employ (II.2) for a four-nucleon composite particle in the entrance and exit channels. As a result we obtain

$$T_{\alpha\beta} = T_{\text{direct}} + T_{\text{ex}}^{(1)} + T_{\text{ex}}^{(2)} + T_{\text{ex}}^{(3)} + T_{\text{ex}}^{(4)}\,. \tag{II.5}$$

The various terms in (II.5) represent, with an obvious notation, the direct term, the single-particle exchange, and the two-, three-, and four-particle exchange terms: Denoting $n_\alpha = n_\beta = n$, we have

$$\begin{aligned}
T_{\text{direct}} &= \langle \Psi_b(1,2,3,4)\Psi_\beta(5,\ldots N)\chi_\beta^{(-)}(\vec{r}_\beta, \vec{k}_f), (V_\beta - U_\beta)\Psi_a(1,2,3,4)\Psi_\alpha(5,\ldots N)\chi_\alpha^{(+)}(\vec{r}_\alpha, \vec{k}_i)\rangle\,,\\
T_{\text{ex}}^{(1)} &= -\binom{4}{1}\binom{n}{1}\langle \Psi_b(1,2,3,4)\Psi_\beta(5,\ldots N)\chi_\beta^{(-)}, (V_\beta - U_\beta)\Psi_a(5,2,3,4)\Psi_\alpha(1,6,\ldots N)\chi_\alpha^{(+)}(\vec{r}_\alpha, \vec{k}_i)\rangle\,,\\
T_{\text{ex}}^{(2)} &= +\binom{4}{2}\binom{n}{2}\langle \Psi_b(1,2,3,4)\Psi_\beta(5,\ldots N)\chi_\beta^{(-)}, (V_\beta - U_\beta)\Psi_a(5,6,3,4)\Psi_\alpha(1,2,7,\ldots N)\chi_\alpha^{(+)}(\vec{r}_\alpha, \vec{k}_i)\rangle\,,\\
T_{\text{ex}}^{(3)} &= -\binom{4}{3}\binom{n}{3}\langle \Psi_b(1,2,3,4)\Psi_\beta(5,\ldots N)\chi_\beta^{(-)}, (V_\beta - U_\beta)\Psi_a(5,6,7,4)\Psi_\alpha(1,2,3,8,\ldots N)\chi_\alpha^{(+)}(\vec{r}_\alpha, \vec{k}_i)\rangle\,,\\
T_{\text{ex}}^{(4)} &= +\binom{4}{4}\binom{n}{4}\langle \Psi_b(1,2,3,4)\Psi_\beta(5,\ldots N)\chi_\beta^{(-)}, (V_\beta - U_\beta)\Psi_a(5,6,7,8)\Psi_\alpha(1,2,3,4,9,\ldots N)\chi_\alpha^{(+)}(\vec{r}_\alpha, \vec{k}_i)\rangle\,.
\end{aligned} \tag{II.6}$$

The binomial coefficients in (II.6) arise from counting the permutations involved. The total number of permutations, regardless of order, between two groups of n_a and n_A objects respectively is $\binom{n_A+n_a}{n_a}$. This number is obtained by adding the unity permutation to the number of permutations permitting the exchange of one object between the groups, two objects etc. The number of permutations where k objects are interchanged, regardless of the order, is clearly $\binom{n_a}{k}\binom{n_A}{k}$. Since the wave functions Ψ in (II.6) are already antisymmetrized, all permutations of one type yield the same matrix element and give rise to the assigned combinatorial factors. In addition, we have

$$\sum_{k=0}^{\min(n_a, n_A)}\binom{n_a}{k}\binom{n_A}{k} = \binom{n_a+n_A}{n_a}\,.$$

Following the formula given by Austern[18] the "knock-on" term is:

$$T(\mathrm{KO}) = \binom{4}{4}\binom{n}{4} \langle \Psi_b(1,2,3,4)\Psi_\beta(5\cdots N)\chi_\beta^{(-)}(\vec{r}_\beta,\vec{k}_f), V(1\cdots 4;\ 5\cdots 8) \times \Psi_a(5,6,7,8)\Psi_\alpha(1\cdots 4, 8\cdots N)\chi_\alpha^{(+)}(\vec{r}_\alpha,\vec{k}_i)\rangle , \tag{II.7}$$

where, for elastic scattering $\Psi_a = \Psi_b$ is the ground-state intrinsic α-particle wave function, $\Psi_\beta = \Psi_\alpha$ represent the target in its ground state, $\vec{r}_\alpha = \vec{r}_\beta$ is the vector between the α-particle center of mass and the target center of mass, and the interaction leading to the "knock-out" process is

$$v(1,\ldots,4;\ 5,\ldots,8) = \sum_{\substack{i=1\cdots 4\\ j=5\cdots 8}} V(i,j) . \tag{II.8}$$

In order to evaluate (II.7) further simplifying assumptions have to be introduced. The dependence of Ψ_α, Ψ_β on the coordinate appearing in the interaction is separated out, and the formalism for developing an expression with which we can obtain an estimate of the knock-out contribution is given in Appendixes I and II.

Using (A II.4), (A II.5), in (A II.3) it follows that;

$$T(\mathrm{KO}) \cong \frac{1}{(4!)^2}\sum_P \langle \Psi_\alpha | A_P^\dagger(\alpha)A_P(\alpha)|\Psi_\alpha\rangle \langle \Phi_P(\vec{R}_1)\chi^{(-)}(\vec{R}_2,\vec{k}_f), V(\vec{R}_1,\vec{R}_2)\Phi_P(\vec{R}_2)\chi^{(+)}(\vec{R}_1,\vec{k}_i)\rangle , \tag{II.9}$$

where $A_P^\dagger(\alpha)$ stands for the operator that creates an α particle with center-of-mass quantum numbers P. The matrix element $\langle \Psi_\alpha | A_P^\dagger(\alpha)A_P(\alpha)|\Psi_\alpha\rangle$ is a spectroscopic amplitude and measures the "number of α's" in the total antisymmetrized wave function Ψ_α.

It is important to note that the normalization of the "spectroscopic amplitudes" in (II.9) is according to (A I.5)

$$\frac{1}{(4!)^2}\sum_{P,Q}\langle \Psi_\alpha^{(N)}|A_{PQ}^\dagger A_{PQ}|\Psi_\alpha^{(N)}\rangle = \frac{1}{(4!)^2}N(N-1)(N-2)(N-3) = \frac{1}{4!}\binom{N}{4} \tag{II.10}$$

which is approximately 3800 for $N=40$. The fraction of sum rule (II.10) absorbed by its "α terms" is, according to the model, the spectroscopic information probed by the ALAS.

If protons and neutrons are treated separately, the above discussion and approximations follow similar lines. Eventually one again derives (II.9), with rule (A I.8)

$$\frac{1}{(2!)^4}\sum_{P,Q}\langle \Psi_\alpha^{(n_p n_n)}|A_{PQ}^\dagger A_{PQ}|\Psi_\alpha^{(n_p n_n)}\rangle = \frac{1}{(2!)^2}\binom{n_p}{2}\binom{n_n}{2} \tag{II.11}$$

which is around 9000 for ^{40}Ca.

To complete the model a recipe for choosing $\Phi_P(R)$, the cluster wave function in the target must be specified. For this we can use a result obtained from the cluster model.[22] If we assume the four particles constituting the α cluster to be in harmonic-oscillator orbits (n_i, l_i) then if all the energy is attached to the center-of-mass motion (n, L) one obtains,

$$2(n-1)+L = \sum_{i=1}^{4}[\,2(n_i-1)+l_i\,] . \tag{II.12}$$

Since we believe these α clusters to exist mainly on the nuclear surface, we choose the (n_i, l_i) levels in the highest major shells occupied, and keep the right-hand side of Eq. (II.11) fixed. In order to actually generate such wave functions, we choose a Woods-Saxon well having a range and depth appropriate to the $(N-4)$ core. This choice can be guided by examining the optical potential obtained by fitting elastic α scattering from the $(N-4)$ target. The binding energy of the cluster to the core is chosen, consistent with this picture, to be the experimental binding energy of an α particle to the $(N-4)$ core. We vary the depth to obtain this energy as an eigenvalue, and the corresponding eigenfunction is the required one. This prescription, although hard to justify rigorously, provides the correct tail for the wave function which is the relevant portion for the α scattering. All other (n, L) states are calculated in the same well, and are therefore more tightly bound. Comparing the exchange amplitude (II.9), (A III.5) with the definition of its partial-wave expansion (I.2) we have

$$a_l = -\frac{4i\mu}{\hbar^2 k}\sum_{nL\lambda}\frac{1}{c}\langle \Psi_\alpha|A_{nL}^\dagger(\alpha)A_{nL}(\alpha)|\Psi_\alpha\rangle \begin{pmatrix} l & \lambda & L \\ 0 & 0 & 0\end{pmatrix}^2 I(l,\lambda,L) \tag{II.13}$$

with

$$I(l,\lambda,L)=\int dR_1 dR_2 f_l(R_1,k)\Phi_{nL}(R_2)v_\lambda(R_1,R_2)\Phi_{nL}(R_1)f_l(R_2,k)\,, \tag{A III.6}$$

where μ is the reduced mass of the α-particle-plus-target system, and

$$c=(4!)^2 \text{ for one type of particle}$$
$$=(2!)^4 \text{ for two types of particles}\,. \tag{II.14}$$

Expression (II.13) summarizes the model. The spectroscopic information appears through the coefficients $\langle\Psi_\alpha|A^\dagger A|\Psi_\alpha\rangle$, which are extracted from experiment.

Spectroscopic amplitudes developed from a detailed nuclear-structure calculation would be energy-independent. The reliability of our calculation can in part be determined by studying the energy dependence of the extracted values.

Let us denote by $\tilde{a}_l$ the contribution resulting from one particular L in (II.13). From expression (A III.6) we see readily that $\tilde{a}_l$ peaks for some l. The argument is the following: For very high l, the centrifugal barrier keeps f_l outside the tail region of bound state Φ_{nL}, and the whole integral is small. For small l, f_l represents a strongly absorbed wave function[18] (in the sense that it oscillates appreciably if the projectile energy is not too low), and the integral will average out to zero. This is equivalent to the observation in inelastic α-particle scattering, calculated in DWBA, that there is no effect caused by cutting out inner contributions in the pertinent radial integrals.

The intermediate l, for which the integral has its maximum value, depends on the bound-state α-particle angular momentum, L. It is known[23] and can be verified directly from (A III.8) that the interaction multipoles v_λ decrease quite rapidly with increasing λ. Therefore, the integral favors low multipoles λ, whereas the strong absorption favors partial waves corresponding to the nuclear surface. Since, however (l,λ,L) in (II.13) must obey the triangle rule, once L is fixed, the maximum value of the integral is determined by these competing trends. If L is low, the maximum will occur for low l. If L is increased, the l for which the integral maximizes, is increased, and will very *roughly* be around L because this situation can utilize the increased magnitudes of the low λ. Therefore, we can find over a range of energies *not too high*, a spike in $\tilde{a}_l$ that fits the data corresponds to a certain L. This L, however, is expected to be *high*. We can understand this feature for wave functions with the same number of nodes on physical grounds. Since the exchange process takes place on the surface, we expect this region of the nucleus to be rich in high-L α particles since they are kept out by the centrifugal barrier whereas the low-L α particles have greater amplitude in the nuclear bulk, where they either "disappear" or do not participate in the reaction. Thus, we expect the high-L α particles to be those which are exchanged.

The maximum L is determined by the target nuclear structure as demonstrated, for example, by Eq. (II.12). Therefore, if the energy is high enough so that the surface partial waves are much greater than L the magnitude of a_l [Eq. (A III.6)] will be greatly diminished. This in turn will lead to a disappearance of ALAS at high energies.

III. RESULTS FOR ^{40}Ca AND DISCUSSION

To apply the formulas of Sec. II we have chosen to calculate the scattering of α particles from ^{40}Ca. The reason for choosing ^{40}Ca ALAS data is primarily the existence of a large quantity of good data for this nucleus at a number of energies.[17,21] The time consumed (~30 min/case on UNIVAC 1108) in each calculation does not permit ready computation of many cases. Furthermore we have in this work attempted to specify only the mechanism of the reaction. Clearly before any significant progress can be made it will be necessary to develop a quantitative nuclear-structure model for surface α particles.

The ingredients of the model are an optical potential that fits the forward-angle cross section ($\theta\lesssim 60^\circ$) where Coulomb and diffraction scattering dominate, a well to generate the bound α states with specified quantum numbers given by (II.12) and binding energy, and the α-α force.

The optical potential was taken from Ref. 24, where it was determined from the scattering of 31-MeV (lab) incident α particles on ^{40}Ca. The parameters are tabulated in Table I. We have used this same potential for all the energies (22–30 MeV) presented in this paper. The choice of the bound-state well is more ambiguous. As a guide, we may conceive a three-body model where the ^{36}Ar core binds an α particle in an effective well, while the incident α particle scatters off this system. Thus, the well that binds the α particle to the ^{36}Ar core should be similar to the *real* part of the optical potential of the α-^{36}Ar elastic scattering. Accordingly, we have taken the Woods-

Saxon parameters of this potential from Ref. 24 and varied the depth to give the correct binding for specified quantum numbers, changing only the radius to reflect a smaller nucleus. For ^{40}Ca, the separation energy is the difference between the bindings of ^{36}Ar and ^{40}Ca and has the value of 7.1 MeV. The parameters of the resulting well are given in Table I. We expect the results of the model not to be sensitve to the particular choice made, since the wave function in the surface region is determined primarily by just the separation energy.

The α-α force has been chosen to have a convenient multipole expansion in Eq. (A II.4). For our purposes, a central Woods-Saxon force[25] is believed to be sufficient instead of an L-dependent one.[26] We have further replaced the force of Ref. 25 by a "best-fit" Gaussian, i.e. we used

$$V_{\alpha\alpha} = -V_0 e^{-\alpha^2(\vec{r}_2 - \vec{r}_1)^2},$$
$$V_0 = 125.\ \text{MeV}, \qquad \alpha = 0.467\ \text{fm}^{-1}. \qquad \text{(III.1)}$$

This Gaussian reproduces the potential of Ref. 25 to within 7% out to better than twice the α-particle half-density radius.

We have investigated the sensitivity of our calculation to the range of the potential (III.1). A variation of the range parameter α by $\pm 20\%$ essentially causes no change in the shape of the differential cross section but does affect the normalization. Varying α from 0.40 to 0.55 fm^{-1} changes the cross section approximately a factor of 3 at the maximum in the cross section at 164°. Since at large angles $d\sigma/d\Omega$ is roughly proportional to N^2 we believe this indicates an accuracy of our normalization to something of the order 50%. The inaccuracies of the model are almost certainly greater than that, considering the quality of the fit to the data.

The double integrals (A II.6) have been performed using the trapezoidal rule with 250 points for each variable in the range 0 to 10 fm. The shape of the bound- and continuum-wave functions indicate this number of points should be adequate.

In the choices described above there are obvious unresolved questions. In this sense it should be appreciated that we do not expect a fit to the data of the quality of a diffraction analysis of forward-angle scattering data.

The only free parameter left in the model is the spectroscopic amplitude in (II.9) which is bounded by (II.10), (II.11), and is *energy-independent*. Thus a consistency check of the model is to reproduce, with the same spectroscopic amplitude, the energy dependence of the ALAS. We have chosen arbitrarily the $E = 29.0$-MeV data[17] to gauge the spectroscopic amplitudes. Two variants were tested: $L = 6$ and $L = 8$ bound α states were used to evaluate $\tilde{a}_l$. The reason for considering just high-L states has been discussed before, and these are the two highest L values allowed by $2s$-$1d$ nucleons. The best-fit spectroscopic amplitudes $N = \langle\Psi_\alpha | A_L^\dagger A_L | \Psi_\alpha\rangle * 1/c$ Eq. (II.14) are given in Table II, and the corresponding differential cross section in Figs. 1 and 2. The spectroscopic amplitudes N in Table II are chosen to yield a good *over-all* fit to the cross-section curve, not just to reproduce the backward-angle region. Trying to fit backward angles better deteriorates the quality of fit at intermediate angles. However, the values of N chosen according to these two criteria are similar. Figures 1 and 2 and Table II exhibit two features:

(1) The spectroscopic amplitude exhausts only a *few percent* of the sum rule [Eqs. (II.10)–(II.11)]. Since we have ignored effects pertaining to the internal structure of the α, distinction between the two sum rules is meaningless. This value for the spectroscopic factor indicates that α-cluster components constitute only a minute part of the nuclear wave function. This conclusion fits the general belief that clusters, if they exist, exist only on the surface therefore exhausting a small fraction of the bulk of the nucleons for ^{40}Ca.

(2) The dramatic effect of including the exchange is appreciated by comparing the OM fit to the calculated one. We note the large rise in backward

TABLE I. Parameters of the optical-model and bound-states Woods-Saxon wells for ^{40}Ca. The potentials appropriate to the distorting potential and the potential binding the α particle in the target nucleus. All well depths are in MeV and all size parameters are in units of 10^{-13} cm.

Specification	V	R_1	a_1	$W_{\text{vol.}}$	R_2	a_2	R_c
Optical model (Reference 24)	50	5.65	0.585	12.4	5.65	0.585	5.65
Bound-state well fitted to give $L=8$ state binding of 7.1 MeV	55	5.45	0.585	0	0	0	5.45

TABLE II. Normalization factors N for $L = 6$ and $L = 8$ determined from the $E_\alpha = 29.0$-MeV data. Fitted $N = \langle\Psi(^{40}\text{Ca}) | A_L^\dagger A_L | \Psi(^{40}\text{Ca})\rangle \frac{1}{c}$ Eq. (II.14) values for $E_{\text{lab}} = 29.$ MeV.

Partial wave L	N
6	300 [a]
8	70

[a] This is the highest value consistent with unitarity of the partial-wave amplitudes.

angles *and* the "lifting" of the intermediate angle region ($90° \lesssim \theta \lesssim 130°$). These two features are characteristic of the data and are clearly missing in the OM calculation which fits the forward angles.

As to the detailed fit to the data we note that the calculation of Fig. 1 is not quite in phase with the experimental results. The periodicity seems too small by a few degrees. This motivated us to examine the $L=6$ α cluster since we expect, roughly speaking, a periodicity of $\pi/(2l+1)$ where l is the angular momentum of a sharp spike. Since decreasing L decreases the spike's "l," we hoped this cluster wave would fit better. It is clear from Fig. 2 that the $L=6$ contribution makes a negligible improvement to the periodicity, and, when made large enough to fit the magnitude at large angles, completely destroys the forward and intermediate angle agreement. A mixture of $L=6$ and $L=8$ contribution does not significantly differ when reasonable amplitudes for the two contributions are used.

The shape of the angular distribution at large angles is influenced by the width of the spike as well as its location. From (A III.6) we can see that the range of the effective α-α potential will strongly influence this width. Since there are many questions concerning the use of the potential (IV.1) we feel the phase discrepancies are not overly serious. In this context it should be noted that the odd multipoles of v_λ are not equal to zero.

In Fig. 3 we have depicted the absolute value of partial-wave amplitudes, for $E=29$ MeV and tabulated them in Table III. We note clearly the spike in $|\tilde{a}_l|$ though in the sum of the $|N\tilde{a}_l+\eta_l^{(\mathrm{opt})}|$ the spike is sitting on the edge of the "slope" of the rising optical-potential amplitudes. As the energy is lowered, as shown in Fig. 4 for $E_\alpha=24$ MeV, the $\tilde{a}_l$ "spike" does not shift as rapidly as the $\eta_l^{(\mathrm{opt})}$ and therefore tends to be "buried" by $\eta_l^{(\mathrm{opt})}$. We note that the spike shows up as a change in the "slope" of the total η_l, which directly affects the delicate cancellations that take place at backward angles.

Another point of interest is the "height" of the spike in $N|\tilde{a}_l|$. Phenomenological OM fits[1] of the ALAS reveal a spike of about 0.1 in height. This order of magnitude is indeed reproduced by the $L=8|\tilde{a}_l|$'s (Table III) but not by one with reasonable parameters for $L=6$. This is another indication that, within this model, $L=8$ α cluster participate the reaction. In fact with $L=6$ the normalization of $N=300$ comes close to the limits dictated by unitarity ($\eta_l \leq 1$).

An important check of the model is the energy variation it predicts. These results are presented in Fig. 5 where we have shown the cross section for $E=24$ MeV. The angular distributions in Figs. 1 and 5 show the comparison with experiment of our calculation with $N=70$ and a fixed OM distorting potential which was not varied with energy. It can be seen from Fig. 5 that some of the energy

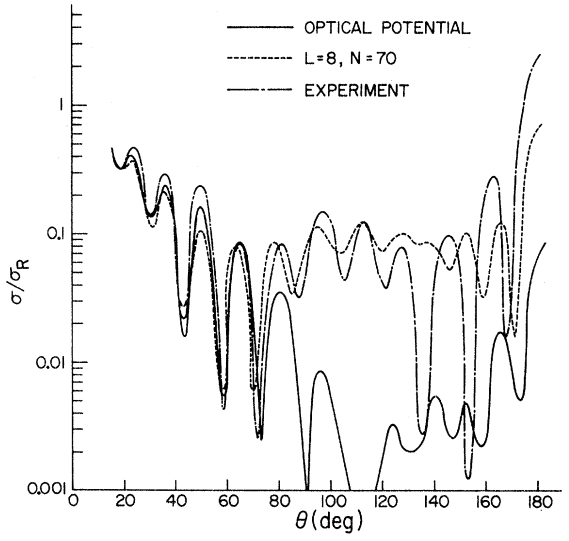

FIG. 1. The differential cross section plotted as the ratio to point-charge scattering, for the scattering of 29.0-MeV α particles from ^{40}Ca. The experimental data are from Ref. 17. The curve labeled $L=8, N=70$ is the curve calculated by adding an amplitude arising from the KO exchange process to the OM amplitude in calculating the cross section. The OM contribution by itself is also shown.

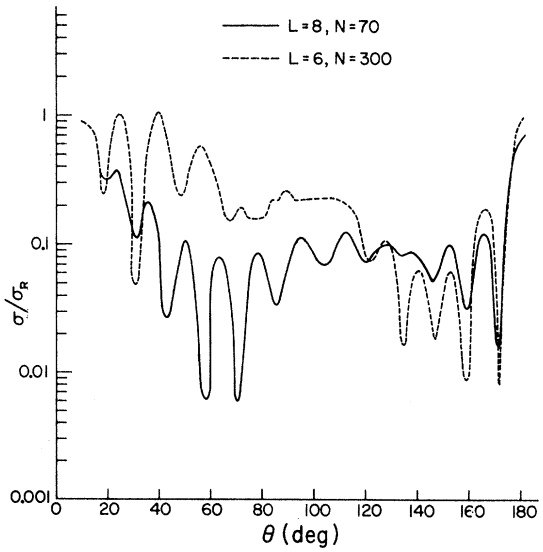

FIG. 2. The calculated cross section for an $L=6$ spike and the $L=8$ spike with normalization appropriate to the large-angle cross sections.

dependence of the scattering might be incorporated into the normalization factor. However, such effective energy dependence is clearly inadequate.

We have also calculated the cross section for $E_\alpha = 22.0$ MeV. In this case disagreement with experiment is significant. However, we observe that in the experiment[17] the cross section at the largest angle (176°) as a function of energy varies as 5.98:7.71:26.2 for $E_\alpha = 29$, 24.1, and 22 MeV. Figures 1 and 5 show a slow increase in the calculated cross sections with decreasing energy consistent with the 29.0- and 24.1-MeV data. We see no simple explanation for the sudden increase at 22.0 MeV except the onset of a new phenomenon such as a compound nuclear resonance.

In Fig. 6 we show our calculated energy dependence for the cross section integrated from 100 to 180°. The limits of integration were chosen to eliminate the Coulomb part of the cross section and cover the ALAS part. This result is in qualitative agreement with the data of Refs. 1, 17, and 21 showing essentially a disappearance of ALAS, at least as characterized by pronounced large-angle cross section, with increasing energy.

IV. DISCUSSION AND COMPARISON WITH OTHER RESULTS

There have been a number of both qualitative and quantitative explanations attempting to explain the ALAS. Generally they have fallen into two classes reminiscent of some of the simple ideas of duality in particle physics.

The first of these classes, essentially, attempts to explain the effect in terms of entrance-channel phenomena. The back-surface reflection,[6] Regge-pole-like spikes in η_l vs l,[7, 8, 12, 13] and l-dependent optical potential[5] fall into this category. The common ingredient of all these optical descriptions can be as a modification of the usual OM S matrix for l values near those for which $\eta_l \sim \frac{1}{2}$. Our approach has in essence accepted the qualitative validity of these descriptions but has argued that while they may be correct they offer little or no insight to a microscopic description of the process. This statement is only partially true, however. The l-dependent potential of Eberhard[5] justifies its existence by reference to the angular momenta available at a given energy in single-particle motion and argues

TABLE III. Partial-wave amplitudes for $E_\alpha = 29$ MeV (lab). The partial-wave amplitudes as a function of l. The first column $\tilde{a}_l$ are the real and imaginary parts of the amplitude given by Eq. (II.18) with $N=1$ and $L=8$. The second set has $L=6$. The third set is the optical-model partial-wave amplitudes. The fourth set is the complete amplitude. For comparison we also show the direct term, Eq. (A III.1). The entries are of the form $s \times aa - n$ where s is the sign of the amplitude; aa the value and $-n$ the exponent (base 10) i.e., real part $\tilde{a}_{l_3} = -0.12 \times 10^{-2}$.

	$\tilde{a}_l$ $L=8$		$\tilde{a}_l$ $L=6$		$\eta_l^{(\mathrm{opt})}$		$N\tilde{a}_l + \eta_l^{(\mathrm{opt})}$ $L=8$		$\tilde{a}_l^{(\mathrm{di})}$ $L=8$	
l	Real	Imaginary	Real	Imaginary	Real	Imaginary	Real	Imaginary	Real	Imaginary
0	0.29 − 5	−0.21 − 6	0.53 − 4	0.11 − 4	−0.013	0.013	−0.012	0.013	0.38 − 5	0.23 − 5
1	−0.59 − 5	−0.18 − 5	−0.10 − 3	−0.28 − 4	0.023	0.002	0.023	0.001	−0.13 − 5	0.36 − 5
2	0.11 − 5	0.56 − 5	−0.10 − 4	0.85 − 4	−0.006	−0.017	−0.005	−0.017	−0.30 − 5	0.26 − 5
3	0.14 − 4	0.36 − 6	0.21 − 3	0.21 − 5	−0.025	0.006	−0.024	−0.006	0.28 − 5	0.31 − 5
4	−0.22 − 5	−0.18 − 4	0.42 − 4	−0.23 − 3	−0.001	0.018	−0.001	0.017	0.37 − 5	−0.23 − 5
5	−0.41 − 4	−0.15 − 4	−0.48 − 3	−0.18 − 3	0.028	0.004	0.025	0.003	−0.12 − 5	−0.45 − 5
6	−0.34 − 4	0.52 − 4	−0.60 − 3	0.63 − 3	0.021	−0.013	0.018	−0.010	−0.50 − 5	−0.30 − 5
7	0.10 − 3	0.11 − 3	0.11 − 2	0.13 − 2	−0.021	−0.013	−0.014	−0.006	−0.20 − 5	0.49 − 5
8	0.24 − 3	−0.10 − 3	0.28 − 2	−0.63 − 3	−0.046	0.000	−0.029	−0.007	0.42 − 5	0.36 − 5
9	−0.21 − 3	−0.50 − 3	0.11 − 2	−0.30 − 2	−0.006	−0.001	−0.020	−0.036	0.46 − 5	−0.33 − 5
10	−0.11 − 2	0.32 − 3	−0.15 − 2	−0.19 − 2	0.074	−0.039	−0.004	−0.016	−0.27 − 5	−0.49 − 5
11	0.37 − 3	0.18 − 2	−0.15 − 2	0.70 − 4	0.117	−0.043	0.143	0.081	−0.44 − 5	0.26 − 5
12	0.18 − 2	−0.84 − 3	−0.58 − 3	0.60 − 3	0.196	0.108	0.324	0.049	0.30 − 5	0.27 − 5
13	−0.12 − 2	−0.70 − 3	−0.35 − 4	0.68 − 3	0.455	0.258	0.374	0.209	0.89 − 7	−0.21 − 5
14	0.16 − 3	0.39 − 3	0.43 − 3	0.59 − 5	0.740	0.275	0.751	0.301	−0.27 − 6	0.44 − 6
15	0.29 − 4	−0.28 − 4	0.14 − 4	−0.77 − 4	0.925	0.160	0.927	0.158	0.40 − 7	0.88 − 9
16	−0.27 − 6	−0.35 − 5	−0.43 − 5	−0.10 − 4	0.975	0.074	0.975	0.073	0.0	0.0
17	−0.18 − 6	−0.35 − 6	−0.11 − 5	−0.15 − 5	0.990	0.034	0.990	0.034	0.0	0.0

that the lack of a sufficient density of single-particle states with adequate angular momenta should cause a decrease in the absorption potential for high partial waves. While this is physically reasonable it only provides a basis for understanding the cut-off l value and not the additional parameters necessary to fit the data, especially the width in l space, of the l-dependent function used to describe the absorptive potential. Specific objections to an l-dependent optical potential have been raised by Oeschler *et al.*[3] and Schmeing.[17] These objections are valid though they in turn can be countered in several ways. These counter proposals, while removing the simplicity of interpretation suggested by Eberhard, might in fact, enable the data to be fitted albeit with isotope-dependent parameters.

As was pointed out by McVoy[7] and recently emphasized by Rinat[12] the Regge-like description of the ALAS may shed light on the nuclear process involved in ALAS. In their view a family of states whose trajectory was capable of being described by a set of fixed quantum numbers, which differed only in the angular momentum, would give rise to a Regge-like description. Such a trajectory would be, for example, a highly excited rotational band where the energy of the states varies as $L(L+1)$. We would caution that an $L(L+1)$ behavior of the ALAS peaking *may* not reflect anything more than strong absorption. For example, if strong absorption dominates medium-energy α-particle reactions then the crucial L value pertaining to large angle is $L_0 \sim kR$, this varies as $E^{1/2}$, therefore $E \sim L_0^2$ and therefore one gets behavior similar to a rotational spectrum, without necessarily having any underlying rotational structure present. To develop the rotational picture in a Regge-like framework would, it seems to us, entail being

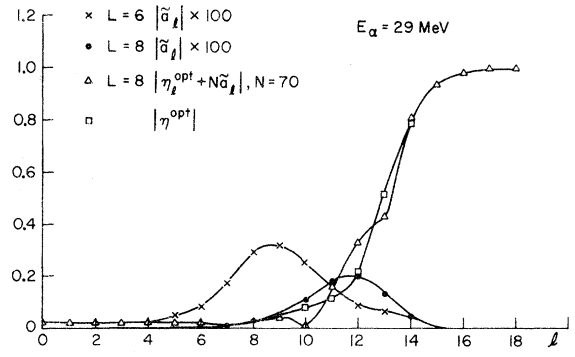

FIG. 3. For an α particle of 29.0 MeV the amplitude of the OM contribution to the S matrix as well as the contributions from an $L=6$ and $L=8$ bound α-particle KO process are shown. Also shown is the over-all S matrix as a function of l, the incident orbital angular momentum.

able to understand the magnitudes of residues of the poles at the very least. Furthermore if we plot, on an Argand diagram the exchange amplitude $\tilde{a}_l$, as shown in Fig. 7, we see that the trajectory, as a function of l, does in fact rotate clockwise as do the Regge trajectories shown by McVoy. We therefore have an interpretation consistent with the Regge formulation without specifically introducing a pole-dominant term. In other words, our interpretation could be said to provide a microscopic derivation of the important Regge poles in this reaction.

The other category of interpretations, into which ours falls, involve invoking an α-α interaction.[27] The calculation nearest to ours in spirit is that of Thompson.[14] We disagree with his conclusion that only low partial waves in the α-α system enter the calculation. We also disagree with his neglect of the quantitative role of antisymmetrization, and relation of the exchange process to the $(\alpha, 2\alpha)$ reaction at much higher energy.

An early attempt to understand the ALAS in terms of an α-α interaction was made by Schmeing.[11] The term she evaluated was essentially our direct term (see Appendix III) which shows no peaking in l space as can be seen from Table I. Equations (A IV.3) shows that the combinational factors arising in the antisymmetrization in fact cause the direct term to be negligible despite better overlap in the matrix elements.

References 2 and 3 emphasize the role of specific clustering effects in determining ALAS. Our calculation obviously utilizes the particularly stable α configuration as described in Sec. II. Since α clustering must be a surface effect and should not involve all A nucleons in the target we expect our empirical normalization to be small compared to the sum-rule limits Eq. (II.15). In fact our normalization is such that if all 20 neutrons and 20 protons were involved in this single configuration the spectroscopic factor would be $\binom{20}{2}^2 \sim 4\times 10^4$ whereas to fit the large angles we re-

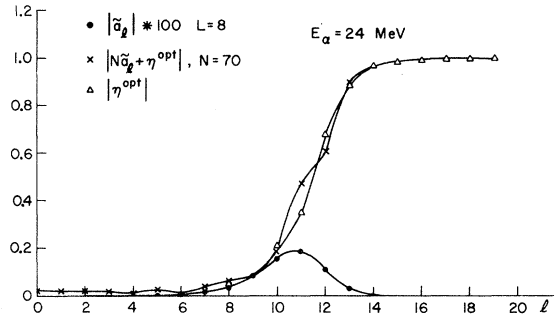

FIG. 4. Same as Fig. 3 except that E_α=24.0 MeV.

quire only a normalization of order 70 which is equal to between $(\frac{4}{2})^2$ and $(\frac{5}{2})^2$, confirming our suspicion that only a few outer nucleons participate in the interaction. We speculate that it is just the relatively small number of nucleons which makes the model sensitive to the shell-model structure of the nucleus in the sense of Ref. 3. While we have not specifically calculated any isotopic effects we believe we have developed a procedure for incorporating such spectroscopic information into its role in elastic α-particle scattering. To illustrate this we point out that the increased size of ^{44}Ca[28] means that $\eta_l \sim \frac{1}{2}$ will be at higher l value at the same time that the increased separation energy of the last α particle (8.84 MeV for ^{44}Ca compared to 6.25 for ^{42}Ca), along with any blocking or other specific nuclear effects, would result in a much lower value for the radial integral (A III.6).

Our formulation of the KO contribution to elastic scattering also provides a ready explanation of the inelastic scattering results of Schmeing and Santo.[29] The width of the spike in the case that initial and final angular momenta are different will be increased because of the wider range of multipoles λ of the α-α force. As the width of the spike increases the opposing phases of the nearby Legendre polynomials at large angles it will cause an averaging which will tend to wash out any particular enhancement at these angles.

While we have not considered "core-exchange" terms other attempts to fit lighter-element experiments showing ALAS have been made. For $\alpha + ^{16}$O Noble and Coelho[10] have considered heavy-particle stripping. It is not clear to us that their treatment of the absorption or the treatment of the Pauli principle was accurate enough to lend significance to their spectroscopic factors which, while less than unity, were quite high.

It has been suggested by Austern[30] that in heavier nuclei the core-exchange terms might in fact be small. In this context it may be that the recent data by Sewell *et al.*[31] showing a "resonance"-like behavior for 180° scattering from nuclei heavier than ^{40}Ca may be consistent with our interpretation. While we have not performed any specific calculation the energy width of their structure is similar to that shown in Fig. 6.

On the other hand we obviously cannot rule out HPS or simple compound-nuclear resonances in the case of light nuclei such as ^{16}O. In fact, as seen for example in the data of Cowley and Heymann,[31] the large-angle cross section is comparable to that at forward angles even for energies such that the Coulomb effects are relatively important at forward angles as they are in the case of ^{40}Ca. An α-particle resonance with an appreciable fraction of the Wigner limit for its width could fit such data and might explain why the light nuclei have different qualitative behavior from the Ca data. Consistent with this should also be noted that the "spikes" introduced by Cowley and Heymann are large compared to those we utilize. In fact some of their energies have $a_l \sim 1$ for the spike whereas our $N\bar{a}_l \sim 0.1$. Of course in their case the Regge description is only a representation of the observed structure and may very well represent only compound-nucleus properties.

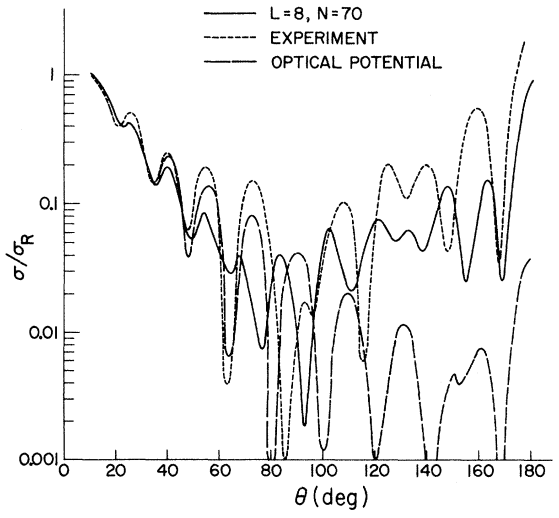

FIG. 5. Same as Fig. 1 except that $E_\alpha = 24.0$ MeV.

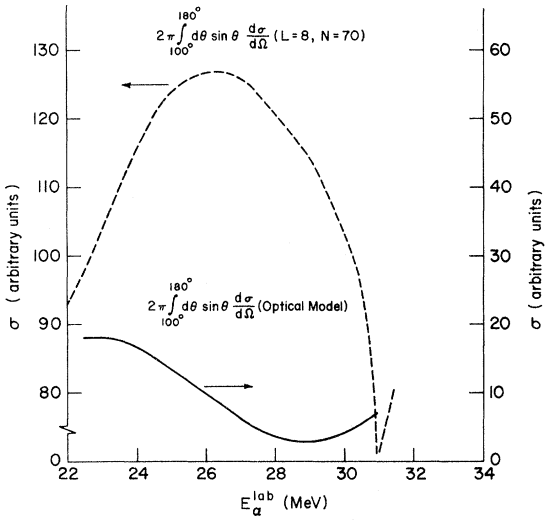

FIG. 6. The integrated cross section from 100 to 180° as a function of the energy for the OM without an exchange contribution and for the complete calculation showing the decrease of the exchange term with increasing energy. The units are arbitrary but are the same for both curves.

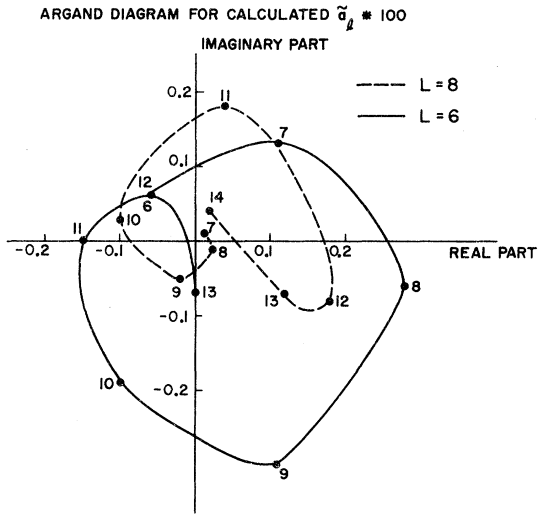

FIG. 7. The Argand diagram for the exchange contribution to the scattering amplitude for both the $L=6$ and $L=8$ bound states as a function of orbital angular momentum. In both cases the trajectory circulates clockwise with increasing l.

V. CONCLUSIONS

We have shown that a DWBA analysis of the KO exchange term, added to the amplitude for elastic scattering as derived from the OM, provides a reasonable fit to the intermediate- and large-angle elastic scattering of α particles from ^{40}Ca. The optical parameters are determined by fitting only forward-angle scattering data. The spectroscopic amplitude used to normalize the DWBA amplitude to experiment is sufficiently small so as not to seriously upset the forward-angle contribution while producing large changes at intermediate and backward angle. We also argue that the analysis is consistent with isotopic effects, and the observed energy dependence.

Comparisons are made with other explanations of the ALAS and it is shown that essentially most of these explanations are consistent with the results obtained in this work. In the case of the Regge-pole explanation we have provided a possible microscopic derivation of the pole.

That aspect obviously needing further analysis involves the cluster spectroscopy of nuclei demonstrating ALAS. The "core-exchange" contributions should also be evaluated.

ACKNOWLEDGMENTS

We would like to thank Professor Avraham Rinat for a series of critical and stimulating discussions. Tom White of the University of Maryland and Amnon Moalem of Tel-Aviv University were of extremely valuable assistance in the computational aspects of this problem. We would also like to thank H. Schmeing for making his data available to us.

One of the authors (D.A.) would like to thank the Center for Theoretical Physics of the University of Maryland for making his stay at Maryland possible, and the other (N.S.W.) would like to thank the Weizmann Institute and Tel-Aviv University for assistance while in Israel.

Computing time, in large quantities, was supplied by Computer Science Center of the University of Maryland and Tel-Aviv University and the Weizmann Institute.

APPENDIX I

The formulas derived below concern the cofactor expansion of an antisymmetrized wave function and sum rules obeyed by spectroscopic amplitudes. We assume, first, one kind of particles for simplicity.

Denote by $a_\alpha^\dagger, a_\alpha$ fermion creation and annihilation operators for a single-particle state α. The number operator $\hat{N}$ in the space of antisymmetric wave functions is

$$\hat{N}=\sum_\alpha a_\alpha^\dagger a_\alpha . \tag{A I.1}$$

Employing the fermion anticommutation relation, one easily proves

$$\begin{aligned}
&\sum_{\alpha\beta} a_\alpha^\dagger a_\beta^\dagger a_\beta a_\alpha=\hat{N}(\hat{N}-1),\\
&\sum_{\alpha\beta\gamma} a_\alpha^\dagger a_\beta^\dagger a_\gamma^\dagger a_\gamma a_\beta a_\alpha=\hat{N}(\hat{N}-1)(\hat{N}-2),\\
&\sum_{\alpha\beta\gamma\delta} a_\alpha^\dagger a_\beta^\dagger a_\gamma^\dagger a_\delta^\dagger a_\delta a_\gamma a_\beta a_\alpha=\hat{N}(\hat{N}-1)(\hat{N}-2)(\hat{N}-3).
\end{aligned} \tag{A I.2}$$

The various lines in (A I.2) express the pair-number operator to the quartet-number operator.

The spectroscopic amplitude introduced below does not coincide with the standard one in that the normalization is different and angular momentum coefficients are omitted. For our particular purpose, however, it will be sufficient. Denote by $\Psi_f^{(N)}$ an antisymmetrized state with N particles, then the single-particle

spectroscopic amplitude $S^{(N)}_{f(\alpha)i}$ is defined by

$$S^{(N)}_{f(\alpha)i} = \langle \Psi^{(N)}_f, a^\dagger_\alpha \Psi^{(N-1)}_i \rangle . \tag{A I.3}$$

By the same token, two- and four-particle spectroscopic amplitudes can be defined similarly

$$S^{(N)}_{f(\alpha\beta)i} = \langle \Psi^{(N)}_f, a^\dagger_\alpha a^\dagger_\beta \Psi^{(N-2)}_i \rangle,$$
$$S^{(N)}_{f(\alpha\beta\gamma\delta)i} = \langle \Psi^{(N)}_f, a^\dagger_\alpha a^\dagger_\beta a^\dagger_\gamma a^\dagger_\delta \Psi^{(N-4)}_i \rangle . \tag{A I.4}$$

Using closure and (A I.2) the following sum rules follow easily:

$$\sum_i |S^{(N)}_{f(\alpha)i}|^2 = \langle \Psi^{(N)}_f, a^\dagger_\alpha a_\alpha \Psi^{(N)}_f \rangle ,$$
$$\sum_{i\alpha} |S^{(N)}_{f(\alpha)i}|^2 = N ,$$
$$\sum_{i\alpha\beta\gamma\delta} |S^{(N)}_{f(\alpha\beta\gamma\delta)i}|^2 = \sum_{i\alpha\beta\gamma\delta} \langle \Psi^{(N)}_f, a^\dagger_\alpha a^\dagger_\beta a^\dagger_\gamma a^\dagger_\delta a_\delta a_\gamma a_\beta a_\alpha \Psi^{(N)}_i \rangle$$
$$= N(N-1)(N-2)(N-3) . \tag{A I.5}$$

In the sum rules (A I.5) we have deliberately taken absolute values to include scattering states in the closure relation.

The cofactor expansion of an antisymmetrized wave function $\Psi^{(N)}_f$ follows easily from (A I.5) and (A I.2). If ϕ_i denotes a single-particle orbital member of a complete set, we have

$$\Psi^{(N)}_f = \frac{1}{\sqrt{N}} \sum_\alpha \phi_\alpha(x_1)^* [\, a_\alpha \Psi^{(N)}_f]$$
$$= \frac{1}{2!} \frac{1}{\sqrt{\binom{N}{2}}} \sum_{\alpha\beta} \tilde{A}\, [\, \phi_\alpha(x_1)\phi_\beta(x_2)]\, [\, a_\alpha a_\beta \Psi^{(N)}_f]$$
$$= \frac{1}{4!} \frac{1}{\sqrt{\binom{N}{2}}} \sum_{\alpha\beta\gamma\delta} \tilde{A}\, [\, \phi_\alpha(x_1)\phi_\beta(x_2)\phi_\gamma(x_3)\phi_\delta(x_4)]^* [\, a_\alpha a_\beta a_\gamma a_\delta \Psi^{(N)}_f] . \tag{A I.6}$$

In (A I.6), $\tilde{A}$ is the normalized antisymmetrization operator of N objects

$$\tilde{A} = \frac{1}{\sqrt{N!}} \sum_P (-1)^P P_N . \tag{A I.7}$$

Formulas (A I.6) express merely the expansion theorem of a determinant by one, two, or four rows. Therefore any labeled particle coordinate can be separated this way.

The above discussion is easily carried over to the case of two kinds of particles, p and n. In this case we have in particular

$$\sum_{(\alpha\beta)_p(\gamma\delta)_n} \langle \Psi^{(n_p n_n)}_f, a^\dagger_{\alpha_p} a^\dagger_{\beta_p} a^\dagger_{\gamma_n} a^\dagger_{\delta_n} a_{\delta_n} a_{\gamma_n} a_{\beta_p} a_{\alpha_p} \Psi^{(n_p n_n)}_f \rangle = n_p (n_p - 1)\, n_n (n_n - 1) , \tag{A I.8}$$

where n_p and n_n is the number of protons and neutrons. In addition

$$\Psi^{(n_p n_n)}_f = \frac{1}{(2!)^2 [\binom{n_p}{2}\binom{n_n}{2}]^{1/2}} \sum_{(\alpha\beta)_p(\gamma\delta)_n} \tilde{A}\, [\, \phi_\alpha(x_1)\phi_\beta(x_2)\phi_{\gamma_n}(x_3)\phi_{\delta_n}(x_4)]^* \, {}^*[\, a_{\alpha_p} a_{\beta_p} a_{\gamma_n} a_{\delta_n} \Psi^{(n_p n_n)}_f] . \tag{A I.9}$$

APPENDIX II

The formalism of these Appendixes in essence defines a cluster representation of the interaction in which the bound α-particle cluster interacts with the incident cluster through an effective interaction. Using the cofactor expansion (A I.6) with notation of Appendix I one obtains:

$$T(\mathrm{KO}) = \frac{1}{(4!)^2} \sum_{\substack{\alpha\beta\gamma\delta \\ \alpha'\beta'\gamma'\delta'}} \langle \Psi_A |\, a^\dagger_\alpha a^\dagger_\beta a^\dagger_\gamma a^\dagger_\delta a_{\delta'} a_{\gamma'} a_{\beta'} a_{\alpha'} \,| \Psi_A \rangle \langle \Psi_a(1,\ldots,4) \tilde{A}[\, \phi_\alpha(x_5)\phi_\beta(x_6)\phi_\gamma(x_7)\phi_\delta(x_8)]$$
$$\times \chi^{(-)}_\beta(\vec{r}_\beta, \vec{k}_f) |\, V(1,\ldots,4;5,\ldots,8) \,| \Psi_a(5,\ldots,8) \tilde{A}[\, \phi_{\alpha'}(x_1)\phi_{\beta'}(x_2)\phi_{\gamma'}(x_3)\phi_{\delta'}(x_4)]\, \chi^{(+)}_\alpha(\vec{r}_\alpha, \vec{k}_i) \rangle . \tag{A II.1}$$

Expression (A II.1) is still exact in that the summation is over a complete set of four-particle wave func-

tions. We note, as mentioned in the text, that if the same cofactor expansion is used, the other exchange terms in (II.6) for N large enough are strongly suppressed. We assert now, as part of the model, that the α-cluster terms in (A II.1) dominate the sum. Stated differently, if instead of an uncorrelated four-body wave function basis, we consider *correlated quartets,* the important terms in (A II.1) are the correlation with the same spin and parity as the α particle. The intuitive motivation for this assumption is reminiscent of the cluster model.

Quantitatively, these ideas can be formulated by transforming (A I.4) by a unitary transformation U to a correlated basis, e.g. all eigenfunctions of the four-body Hamiltonian:

$$a_\alpha^\dagger a_\beta^\dagger a_\gamma^\dagger a_\delta^\dagger = \sum_{P,Q} U(\alpha\beta\gamma\delta; PQ) A^\dagger(P,Q) \tilde{A}[\phi_\alpha(1)\phi_\beta(2)\phi_\gamma(3)\phi_\delta(4)] = \sum_{P,Q} U(\alpha\beta\gamma\delta; PQ)\Phi_{PQ}(1,\ldots,4) U U^\dagger = 1 . \tag{A II.2}$$

In (A II.2) P stands for the center-of-mass quantum numbers and Q for the internal relative quantum numbers. The operator $A^\dagger(P,Q)$ creates an antisymmetric cluster with wave function Φ_{PQ}. Inserting (A II.2) in (A II.1) we obtain:

$$T(\mathrm{KO}) = \frac{1}{(4!)^2} \sum_{\substack{P,Q \\ P',Q'}} \langle \Psi_A | A^\dagger(P,Q) A(P',Q') | \Psi_A \rangle$$

$$\times \langle \Psi_a(1\cdots 4)\Phi_{PQ}(5\cdots 8)\chi_\beta^{(-)}(\vec{r}_\beta, \vec{k}_f) | V(1\cdots 4, 5\circ\cdots 8) | \Psi_a(5\cdots 8)\Phi_{P'Q'}(1\cdots 4)\chi_\alpha^{(+)}(\vec{r}_\alpha, \vec{k}_i)\rangle . \tag{A II.3}$$

According to our assumption, we truncate the summation in (A II.3) on Q to include *only* those combinations with α-particle quantum numbers. Thus the relevant Φ_{PQ} in (A II.3) represents an α-cluster having center-of-mass quantum numbers P with respect to an origin in space. If the single-particle states in Ψ are taken as harmonic-oscillator wave functions and, for instance, Ψ_A is a single determinant of the same harmonic oscillator, the Ψ_A center of mass and the Φ_{PQ} center of mass are identical. We shall assume for simplicity this to hold in (A II.3). Thus $\vec{r}_\alpha = \vec{r}_\beta = \vec{R}$ is the center-of-mass coordinate of Φ_{PQ}. Since the target has zero spin, angular momentum conservation gives $P = P'$. We can further simplify (A II.3) by neglecting the internal structure effects of the α's in the scattering process. Thus we assume

$$\Psi_a \approx 1 , \quad \Phi_{PQ} = \Phi_P(\vec{R}) \tag{A II.4}$$

and consistently, the α-α interaction is assumed to depend only on the center-of-mass coordinates

$$V(1,\ldots,4,5,\ldots,8) \cong V(\vec{R}_1, \vec{R}_2) . \tag{A II.5}$$

These simplifications lead to Eq. (II.9).

APPENDIX III

Below we present the angular momentum decomposition of the exchange matrix element (II.9). The interaction (A II.5) is taken to be spin-independent.

$$V(\vec{R}_1, \vec{R}_2) = V(|\vec{R}_1 - \vec{R}_2|) \tag{A III.1}$$

and

$$\Phi_P = \Phi_{nLM} = \frac{\Phi_{nL}(R)}{R} Y_L^M(\Omega_\alpha) \int |\Phi_{nL}|^2 dR = 1 , \tag{A III.2}$$

where n, L denote the principal and angular momentum quantum numbers of the α center-of-mass motion with respect to the core.

Employing the following partial-wave expansions for spinless charged particles[18]

$$|\chi^{(+)}\rangle = \frac{4\pi}{kr} \sum_{lm} i^l e^{i\sigma_l} f_l(k,r) Y_l^m(\Omega_r) Y_l^{*m}(\Omega_k) \langle \chi^{(-)}| = \frac{4\pi}{kr} \sum_{lm} i^{-l} e^{i\sigma_l} f_l(k,r) Y_l^m(\Omega_k) Y_l^{*m}(\Omega_r) \tag{A III.3}$$

and[32]

$$V(|\vec{r}_1 - \vec{r}_2|) = \sum_{\lambda\mu} \frac{4\pi}{2\lambda+1} Y_\lambda^\mu(\Omega_{r_1}) Y_\lambda^{*\mu}(\Omega_{r_2}) v_\lambda(r_1, r_2) \tag{A III.4}$$

we obtain, using standard angular momentum technique ($|k_i| = |k_f| = k$),

$$\langle \Phi_p(\vec{R}_1)\chi^{(-)}(\vec{R}_2, \vec{k}_f), V(\vec{R}_1, \vec{R}_2)\Phi_p(\vec{R}_2)\chi^{(+)}(\vec{R}_1, \vec{k}_i)\rangle$$
$$= \sum_{\mu} \langle \Phi_{nL\mu}(\vec{R}_1)\chi^{(-)}(\vec{R}_2, k_f), V(|\vec{R}_1 - \vec{R}_2|)\Phi_{nL\mu}(\vec{R}_2)\chi^{(+)}(\vec{R}_1, \vec{k}_i)\rangle (L\mu L - \mu|00)^2$$
$$= \frac{4\pi}{k^2} \sum_{\lambda l} e^{2i\sigma l}(2l+1)\begin{pmatrix} l & \lambda & L \\ 0 & 0 & 0 \end{pmatrix}^2 P_l(\cos\theta) I(l, \lambda, L) \qquad \text{(A III.5)}$$

with

$$I(l, \lambda, L) = \int dR_1\, dR_2 f_l(R_1, k)\Phi_{nL}(R_2)v_\lambda(R_1, R_2)\Phi_{nL}(R_1)f_l(R_2, k)\,. \qquad \text{(A III.6)}$$

The extra Clebsch-Gordan coefficient inserted in (A III.5) originates from coupling the cluster Φ_p with the core-wave-function angular momenta to give zero angular momentum to the complete target wave function.

The partial wave expansion (A III.4) for Gaussian force

$$V = -V_0 e^{-\alpha^2(\vec{R}_1 - \vec{R}_2)^2} \qquad \text{(A III.7)}$$

gives[23]

$$v_\lambda(r_1, r_2) = -V_0 e^{-\alpha^2(r_1^2 + r_2^2)}(2\lambda + 1) i_\lambda(2\alpha^2 r_1 r_2)\,, \qquad \text{(A III.8)}$$

where the modified spherical Bessel function i_λ is defined[23]

$$i_\lambda(z) = \left(\frac{\pi}{2z}\right)^{1/2} I_{\lambda+1/2}(z)\,. \qquad \text{(A III.9)}$$

APPENDIX IV

It has been suggested[11] that the ALAS can be interpreted in terms of the direct projectile α-cluster scattering (II.6). Using the same line of derivation and notations as for the exchange term, the result is

$$a_i^{(\mathrm{dl})} = -\frac{4i\mu}{\hbar^2 k} \sum_{Ln} c_1 \langle \Psi_\alpha | A_{nL}^\dagger(\alpha) A_{nL}(\alpha) | \Psi_\alpha \rangle D(l, L)\,, \qquad \text{(A IV.1)}$$

where

$$D(l, L) = \int dR_1\, dR_2 f_l(R_1, k)\Phi_{nL}(R_2)v_0(R_1, R_2)\Phi_{nL}(R_2)f_l(R_1, k) \qquad \text{(A IV.2)}$$

and

$$c_1 = \frac{1}{(4!)^2}\,\frac{1}{\binom{n}{4}} * \frac{n}{4} \quad \text{for one kind of particle}$$
$$= \frac{1}{(2!)^4}\,\frac{1}{\binom{n_p}{2}\binom{n_n}{2}} * (n_p + n_n) \quad \text{for two kinds of particles}\,. \qquad \text{(A IV.3)}$$

The factors in (A IV.3) are determined assuming all pair interactions are equal. We see immediately that the huge combinatorial factors inhibit this kind of mechanism relative to the exchange term.

---

*Work supported in part by the National Science Foundation, Center for Theoretical Physics under Grant No. NSF GU 2061.

†C. T. P. Fellow, University of Maryland.

‡Work supported in part by AEC Contract No. AT-(40-1)-3491. Part of this work was done while on sabbatical leave from the University of Maryland at the Weizmann Institute of Science and the Tel-Aviv University.

[1]C. R. Gruhn and N. S. Wall, Nucl. Phys. **81**, 161 (1966).
[2]G. Gaul *et al.*, Nucl. Phys. **A137**, 177 (1969).
[3]H. Oeschler *et al.*, Phys. Rev. Lett. **28**, 694 (1972).
[4]A. Budzanowski *et al.*, Nucl. Phys. **A126**, 369 (1969).
[5]K. A. Eberhard, Phys. Letters **33B**, 343 (1970).
[6]I. A. Gubkin, Yadern. Fiz. **11**, 598 (1970) [transl.: Sov. J. Nucl. Phys. **11**, 336 (1970)].
[7]K. W. McVoy, Phys. Rev. C **3**, 1104 (1971).
[8]R. Ceuleneer, M. Demeur, and J. Reigner, Nucl. Phys. **82**, 625 (1966); Nucl. Phys. **89**, 177 (1969).
[9]T. Honda, Y. Kudo, and H. Ui, Nucl. Phys. **44**, 472 (1963).
[10]J. Noble and H. Coelho, Phys. Rev. C **3**, 1840 (1971).
[11]N. C. Schmeing, Nucl. Phys. **A142**, 449 (1970).
[12]A. S. Rinat, Phys. Lett. **38B**, 281 (1972).
[13]A. A. Cowley and G. Heymann, Nucl. Phys. **A146**, 465 (1970).
[14]W. G. Thompson, Particles Nuclei **2**, 47 (1971).
[15]A. Brobowski *et al.*, Nucl. Phys. **A126**, 369 (1969).

[16]E. Labie, J. Lega, and P. C. Macq, Nucl. Phys. **A135,** 145 (1969).
[17]H. Schmeing, Ph.D. dissertation, University of Heidelberg, 1970 (unpublished); also see Ref. 1.
[18]N. Austern, *Direct Nuclear Reaction Theories* (Wiley Interscience, New York, 1970).
[19]W. E. Frahn and R. H. Venter, Nucl. Phys. **59,** 651 (1964).
[20]A. Dar and B. Kozlowsky, Phys. Rev. Lett. **15,** 1036 (1965). Also see W. von Oertzen *et al.*, Phys. Lett. **26B,** 291 (1968).
[21]G. Gaul *et al.*, University of Heidelberg report, 1972 (unpublished).
[22]K. Wildermuth, University of Maryland Technical Report No. 281, 1962 (unpublished).
[23]*Handbook of Mathematical Functions*, edited by M. Abramowitz and I. A. Stegun, National Bureau of Standards Applied Mathmatics Series, No. 55 (U.S. GPO, Washington, D.C., 1964), p. 445.
[24]A. Bernstein, in *Advances in Nuclear Physics*, edited by M. Baranger and E. Vogt (Plenum, New York, 1969), Vol. 3.
[25]V. G. Neudatchin *et al.*, Phys. Lett. **34B,** 581 (1971).
[26]S. A. Afzal, A. A. Z. Ahmad, and S. Ali, Rev. Mod. Phys. **41,** 247 (1969).
[27]The application of DWBA transfer processes to elastic scattering has recently been treated by Tobocman, private communication.
[28]R.F. Frosch , Phys. Rev. **174,** 1380 (1968).
[29]H. Schmeing and R. Santo, Nucl. Phys. **33B,** 219 (1971).
[30]Reference 18, especially the discussion of Chapter 10.
[31]P. T. Sewell *et al.*, Phys. Rev. **C 7,** 690 (1973).
[32]A. de-Shalit and I. Talmi, *Nuclear Shell Theory* (Academic, New York, 1963).

PHYSICAL REVIEW C VOLUME 7, NUMBER 4 APRIL 1973

Study of Excited States of ^{14}O by a Particle-Particle Angular-Correlation Technique*

J. G. Pronko
Lockheed Palo Alto Research Laboratory, Palo Alto, California 94304

and

R. G. Hirko† and D. C. Slater
Physics Department, Stanford University, Stanford, California 94305

(Received 11 December 1972)

Excited states of ^{14}O have been investigated with the ^{12}C(^{3}He, n)^{14}O(p)^{13}N reaction at an incident-beam energy of 12 MeV. Proton groups corresponding to ^{14}O excited states were observed in time coincidence with the associated neutrons detected at $\theta_n = 0°$. The natural widths of these states (or limits thereof) were obtained directly from the proton spectrum. Angular-correlation data obtained for these proton groups were analyzed according to a general formalism which allows channel spin as well as orbital angular momentum mixing in the $^{14}O \rightarrow {}^{13}N + p$ exit channel. These analyses yield the following spin and width limitations: [E_x (MeV), J, Γ (keV)]; 5.91, 0 or 1, $\leq$47; 6.29, 2 or 3, 103$\pm$6; 6.59, 2, $\leq$56; and 7.78, 1, 2 or 3, 76$\pm$10. The apparent dominance of a direct-transfer mechanism for the population of these states permits further spin and parity restrictions. Information regarding the wave-function configurations for these states is discussed on the basis of the observed proton decay. Of particular interest is the observance of an f-wave component in the proton decay of the 6.59-MeV state which implies an s^4p^8 (p,f) component in the wave function of that state.

I. INTRODUCTION

Within the mass-14 isobaric triad, the ^{14}O nucleus is the $T_z = -1$ member and has been the least investigated. Figure 1 illustrates the excited states of ^{14}O and some of the known properties as given in the survey article of Ajzenberg-Selove.[1] Most of the information regarding the excited states of ^{14}O have been obtained by means of direct-particle-transfer studies using the ^{12}C(^{3}He, n)^{14}O, ^{14}N(^{3}He, t)^{14}O, and ^{16}O(p, t)^{14}O reactions.[2-6]

For the (^{3}He, n) reaction it is expected that if the reaction proceeds by direct-transfer processes that $T = 1$ and $s = 0$ will be transferred to the excited state in the final nucleus. Two such studies[3,4] were made using this reaction and it was found that indeed it did appear that most of the neutron groups had angular distributions consistent with a two-particle transfer mechanism at the beam energies used. On this assumption and with the use of distorted-wave Born-approximation (DWBA) double-stripping calculations, tentative spin and parity assignments were made.[3,4]

The work with the (^{3}He, t) reaction[5] resulted in probable spin and parity assignments for ^{14}O states based on a comparison of the shapes of the angular distributions with those from transitions